ABBASCHIAN FESTSCHRIFT

Optical study of zinc blend SnS and cubic In$_2$S$_3$:Al thin films prepared by chemical bath deposition

Anis Akkari · Cathy Guasch · Michel Castagne · Najoua Kamoun-Turki

Abstract Multilayers of zinc blend SnS crystalline thin film have been deposited onto glass substrates by a chemical bath deposition (CBD) method. The envelope method, based on the optical transmission spectrum taken at normal incidence, has been successfully applied to determine the layer thickness and to characterize optical properties of thin films having low surface roughness. Optical constants such as refractive index n, extinction coefficient k, as well as the real (ε_r) and imaginary (ε_i) parts of the dielectric constant were determined from transmittance spectrum using this method. Obtained low value of the extinction coefficient in the transparency domain is a good indication of film surface smoothness and homogeneity. To perform the heterojunction structure based on SnS absorber material, cubic In$_2$S$_3$:Al was deposited on SnO$_2$:F/glass as window layer using CBD with different aluminum content. Optical properties of these films were evaluated.

Introduction

Tin sulfide SnS material has been a subject of various recent investigations due to its physical properties and photovoltaic applications [1–3]. This compound belongs to groups IV–VI of compounds formed with Sn as the cation and S as the anion. The constituent elements are nontoxic and abundant in nature leading to the development of devices that are environmentally safe and have public acceptability. Many techniques have been used to produce tin sulfide such as: spray [4, 5], electrodeposition [6], silar method [7], and chemical bath deposition (CBD) [8, 9]. In previous study [8], we have deposited high quality SnS(ZB) films on glass substrates by CBD. This technique which is simple and inexpensive method is useful for large area applications. Optical characterization of SnS and In$_2$S$_3$ thin films can be used as an effective diagnostic tool to assess film quality. The envelope method [10], based on the optical transmission spectrum taken at normal incidence, has been successfully applied to determine the film thickness as well as the optical constants of tin sulfide thin films. To date, envelope method has not yet used for optical characterization of tin sulfide CBD thin films.

In$_2$S$_3$ is a III–VI binary compound. It appears to be one of the most promising candidates for photovoltaics owing to its stability, interesting structural characteristics [11, 12], electronical [13], optical, photoelectrical [14, 15], and acoustical properties [16] as well as its photocatalytic [17] and environmental interest [18].

During the last two decades, indium sulfide and especially β-In$_2$S$_3$ material has been the subject of much research because of its photoconducting behavior which makes it as promising optoelectronic material [19, 20]. Such material can be classified as mid-band gap semiconductor (2.2 eV) as compared to materials such GaAs (1.4 eV, narrow band gap), or to ZnO (3.2 eV, wide band gap) [21, 22]. Nevertheless an efficient photovoltaic structure such as SnS/β-In$_2$S$_3$ requires good structural and optical properties of the β-In$_2$S$_3$ thin layers.

In$_2$S$_3$ exists generally in four phases [23, 24]. Recently, we have shown that β-In$_2$S$_3$ layers can be obtained by the

A. Akkari (✉) · N. Kamoun-Turki
Faculté des Sciences de Tunis El Manar, Laboratoire de Physique de la Matière Condensée, 2092 Tunis, Tunisia
e-mail: anis.akkari@ies.univ-montp2.fr

A. Akkari · C. Guasch · M. Castagne
Institut d'Electronique du Sud, Unité Mixte de Recherche 5214 UM2-CNRS, Université Montpellier II, Place Eugène Bataillon Bat 21 cc083, 34095 Montpellier Cedex 05, France

CBD technique [25, 26]. It is interesting to note that Ag/SnS/β-In$_2$S$_3$/SnO$_2$:F heterojunction [without aluminum (Al) inclusion in the In$_2$S$_3$ film] was elaborated in our laboratory but no photovoltaic effect has been observed.

In this study, to increase the optical band gap of β-In$_2$S$_3$ thin films, Al was introduced in the starting solution. The addition of Al as doping agent in the thin layers of β-In$_2$S$_3$ leads to move the intrinsic absorption of this material toward ultraviolet zone, and therefore to, widen the domain of transmitted wavelength to the absorber material SnS in the SnS/β-In$_2$S$_3$:Al/SnO$_2$:F photovoltaic structure. β-In$_2$S$_3$:Al thin films were deposited on SnO$_2$:F/glass with different concentration ratio $y = \left([\text{Al}^{3+}]/[\text{In}^{3+}]\right) = 0, 20, 30$ and 40%. We have already noticed that in β-In$_{2-x}$Al$_x$S$_3$ prepared by the spray pyrolysis [27], the presence of Al atoms in the material contributes to the growth and to the structure of the deposited films. Moreover it was observed from experiment that the best crystallinity of β-In$_2$S$_3$ was obtained on SnO$_2$/Pyrex substrate; the contamination was also reduced.

In this study, we have also studied the effect of successive deposition runs on the refractive index "n", the extinction coefficient "k", and the real and imaginary parts of the dielectric constant of tin sulfide homogeneous thin layer.

In this way, tin sulfide and indium sulfide thin films have been elaborated on glass substrates and SnO$_2$:F/glass, respectively, with the aim to establish the optimized experimental conditions leading to grown absorber SnS(ZB) and window In$_2$S$_3$:Al thin films with good structural and optical properties such as high SnS absorption coefficient "α" and wide In$_2$S$_3$:Al optical band gap.

To date, the use of CBD multilayers of SnS(ZB) and In$_2$S$_3$:Al as absorber and window material, respectively, to elaborate solar cell Ag/SnS/β-In$_2$S$_3$:Al/SnO$_2$:F has not yet been tested. Haleem et al. [28], have developed and characterized InS$_x$O$_y$(OH)$_Z$/SnS heterojunction; they showed that the photo-response and the conversion efficiency of such cell are still so low.

Experimental details

Deposition of SnS(ZB) absorber layer

Multi-layers SnS thin films have been deposited via CBD process by means of basic solution containing SnCl$_2$·2H$_2$O, diluted triethanolamine (TEA), NH$_4$OH(15 M) as well as thioacetamide (TA) (0.1 M) as precursors. The temperature of the reaction mixture was kept constant using a water bath to 25 °C. The substrates were kept vertically in the hermetically closed deposition bath mounted on a heating magnetic agitator, which controls temperature of the solution. Then, the deposited thin films were taken out

from the bath, washed with water, and finally put in a dried box for approximately 15 min. The Thickness "e" of one layer of SnS is in the order of 100 nm. This value of SnS thin monolayer is rather low [8]. In order to increase the thickness of SnS to be used as an absorber in solar cell we have made multilayer. The thicknesses of the films were evaluated using envelope method as 305, 340, and 455 nm for four, five and six deposition runs, respectively.

Deposition of In$_2$S$_3$:Al window layer

Multilayer indium sulfide thin film has been deposited by a CBD, on SnO$_2$:F/glass substrates with different concentration ratios $y = \left([\text{Al}^{3+}]/[\text{In}^{3+}]\right) = 0, 20, 30$ and 40%. Such SnO$_2$:F films exhibits 75–80% of transparency, and surface resistance of 10–15 Ω/sq [29]. SnO$_2$:F thin layers act as ohmic contact in SnS/In$_2$S$_3$:Al solar cells.

The solution of indium sulfide contains indium chloride and TA as sulfur precursor with concentration (0.1 M). In order to get Al inclusion in β-In$_2$S$_3$ thin films, the necessary mass of AlCl$_3$ are directly added into the deposition solution. Bath temperature is 80 °C; the pH of the solution is controlled to 2 by adding acetic acid into the reaction mixture. The substrates are introduced vertically into the hermetical closed deposition cell. This cell is mounted on a heating magnetic agitator, which controls both temperature and homogeneity of the solution. The bath color leaves clear to yellow. β-In$_2$S$_3$ films nucleated onto submerged surfaces, including beaker walls in about 47 min for one deposition run. The obtained yellow films were taken out from the bath, washed with water, and finally put in a dried box for approximately 15 min [25, 26]. For two deposition runs, we emerged the first obtained thin films in the freshly prepared solution for 47 more min. In this study, we repeat the same bath up to four times with the aim to increase the film thickness.

It is noted that for a number of deposit greater than four times the β-In$_2$S$_3$ thin film collapses, which is caused by the gravitational forces due to the film mass. Gravitational forces affect indeed the forces of adhesion and cohesion between layer and substrate. The similar behavior was observed by Pramanik et al. [30], for orthorhombic SnS thin films grown by CBD on glass substrates during t_d equal to 24 h.

Optical analysis of zinc blend tin sulfide

The optical transmission measurements of zinc blend tin sulfide were obtained by means of a Varian spectrophotometer at room temperature under normal incidence over a large spectral range (0.2–2.5 μm) [8]. Using the

experimental spectra of the optical transmission of our earlier study [8], this study deals with a theoretical simulation of these spectra using the envelope method [10]. Points obtained theoretically allow us to calculate the thickness and optical constants of SnS thin films.
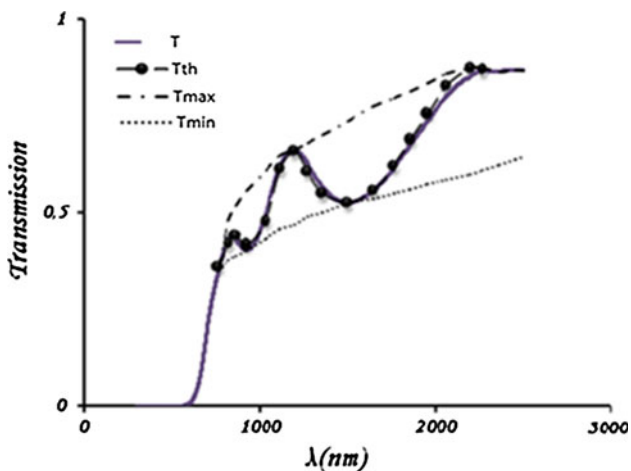
Figure 1 shows both transmission curves experimentally and theoretically for the crystalline SnS(ZB) multilayer formed by six deposition runs. The interference phenomena between the wave fronts generated at two interfaces (air and substrate) defines the sinusoidal behavior of the curves' transmittance in terms of the wavelength. SnS(ZB) thin film exhibits interference fringe pattern in transmission spectrum. This revealed the smooth reflecting surface of the film and there is not much loss of scattering at the surface. Good surface state and homogeneity of the film were confirmed from the appearance of interference fringes in the transmission spectra. The refractive index "n_1" at different wavelengths was calculated in the transparency region using the envelope curve for $T_{max}(\lambda)$ and $T_{min}(\lambda)$ (Fig. 1). The expression for refractive index is given by [10]:

$$n_1 = \left[N + \left(N^2 - n_0^2 n_2^2 \right)^{1/2} \right]^{1/2} \tag{1}$$

with $N = 2n_0 n_2 \left[\frac{(T_{max} - T_{min})}{T_{max} T_{min}} \right] + \left(\frac{n_2^2 + n_0^2}{2} \right)$, n_0 is air refractive index, n_1 is the refractive index of tin sulfide thin film, and n_2 is the refractive index of glass substrate (in our case $n_2 = 1.52$).

The thickness d of tin sulfide layer can be calculated from two maxima or minima using this equation [10]:

$$d = \frac{M \lambda_1 \lambda_2}{2 (\lambda_2 n_1(\lambda_1) - \lambda_1 n_1(\lambda_2))} \tag{2}$$

Fig. 1 Experimentally (T) and theoretically (T_{th}) transmission of zinc blend tin sulfide elaborated by CBD on glass substrates after six depositions runs

where M is the number of oscillations between two extrema ($M = 1$ between two consecutive maxima or minima); λ_1, $n_1(\lambda_1)$ and λ_2, $n_1(\lambda_2)$ are the corresponding wavelengths and refractive index.

Knowing n_1 and d values, the extinction coefficient "k_1" at different wavelengths in the transparency region can be calculated using the following formula [10]:

$$k_1 = \frac{\lambda}{4\pi} \alpha \tag{3}$$

where α is the absorption coefficient given by:

$$\alpha = -\frac{1}{d} \ln(x) \tag{4}$$

and

$$x = \frac{C_1 \left[1 - \left(\frac{T_{max}}{T_{min}} \right)^{1/2} \right]}{C_2 \left[1 + \left(\frac{T_{max}}{T_{min}} \right)^{1/2} \right]},$$

where: $C_1 = (n_1 + n_0)(n_2 + n_1)$ and $C_2 = (n_1 - n_0)(n_2 - n_1)$.

Using the obtained values of refractive index (n_1) and extinction (k_1) coefficient, the real and imaginary parts of dielectric constants are calculated using following expression [29]:

$$\varepsilon_r = n_1^2 - k_1^2 \tag{5}$$

$$\varepsilon_i = 2 n_1 k_1. \tag{6}$$

The thickness of SnS(ZB) multilayers are calculated from Eq. 2. All results are summarized in Table 1. We note that both theoretically thickness values obtained in this study and experimental calculated ones obtained in previously study [8] were already correlated.

The refractive index $n_1(\lambda)$ and the extinction coefficient $k_1(\lambda)$ values were calculated in the transparency domain (750–2500 nm) using Eqs. 1, 3. The variations of $n_1(\lambda)$ and $k_1(\lambda)$ with the wavelength are shown in Fig. 2a, b. It has been found that the refractive index $n_1(\lambda)$ is varying in the range of 2.3–3.2, whereas the extinction coefficient $k_1(\lambda)$ is of the order of 0.05. The low value of extinction coefficient as observed of these films is a qualitative indication of surface smoothness and homogeneity of the films. Subramanian et al. [31] and Koteeswara Reddy et al. [32] are also observed a similar variation of optical parameters in
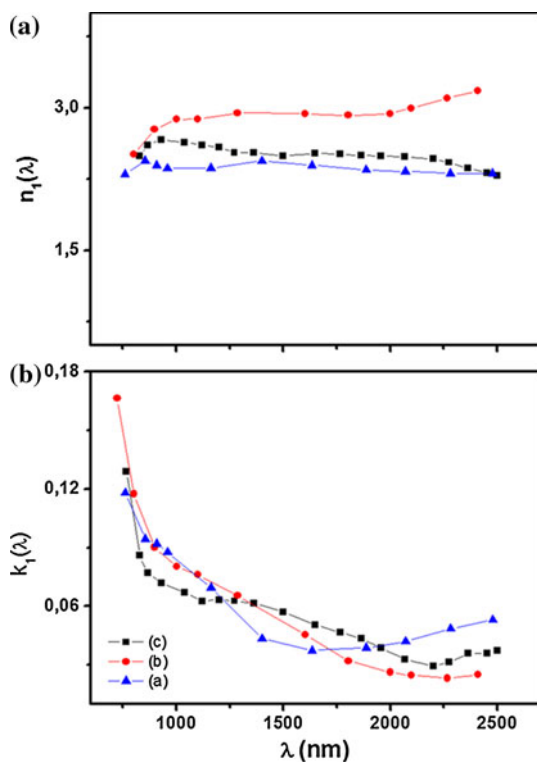
Table 1 Theoretical values of thicknesses of SnS(ZB) multilayer thin film deduced using envelope method

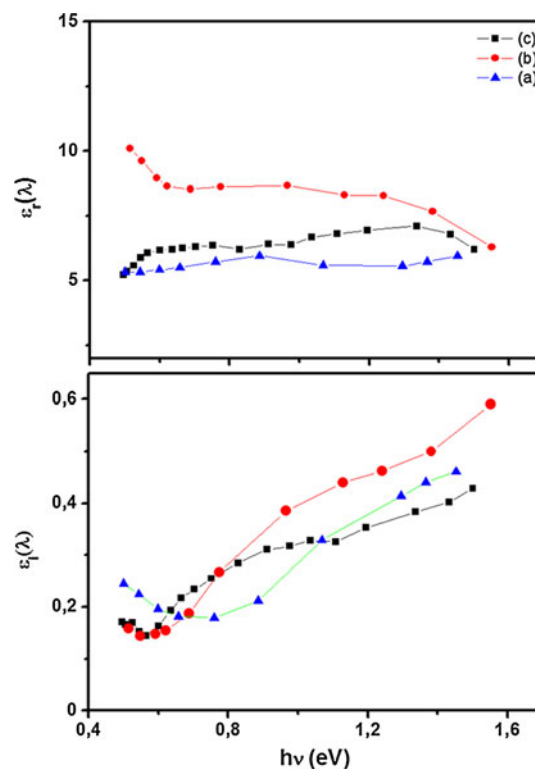| Deposition number	Thickness "d" (nm)
6	455
5	340
4	305

electrodeposition and sprayed deposited SnS thin films. It is clearly show in Fig. 2a that the refractive index obtained in case of five deposition runs of SnS(ZB) is higher than others obtained for four and six deposition runs. This behavior may be due to the existence of an orthorhombic phase revealed by X ray diffraction reported previously [8] which can perturb the refractive index values.

On the other hand, the real (ε_r) and imaginary (ε_i) parts of the dielectric constant ε are related to the n_1 and k_1 values. ε_r and ε_i values were calculated using the Eq. 5, 6. Figure 3 shows ε_r and ε_i values dependence of photon energy. It has been found that the real part of the dielectric constant value of zinc blend tin sulfide thin film remain practically constant with increasing of the photon energy. Also the imaginary part of the dielectric constant value of SnS is found to increase with increasing of the photon energy.

Also, the absorption coefficient α of the SnS(ZB) thin films was determined from transmittance measurements. First, α is calculated in the transparency region using the envelopes method, however, this method is not valid in the strong absorption region. In 450–750 nm domain, α is indeed calculated using the following expression [29]:

Fig. 3 The real (ε_r) and imaginary (ε_i) parts of the dielectric constant ε of SnS(ZB) thin layers grown for four (*a*), five (*b*), and six (*c*) depositions runs versus photon energy (*hv*)
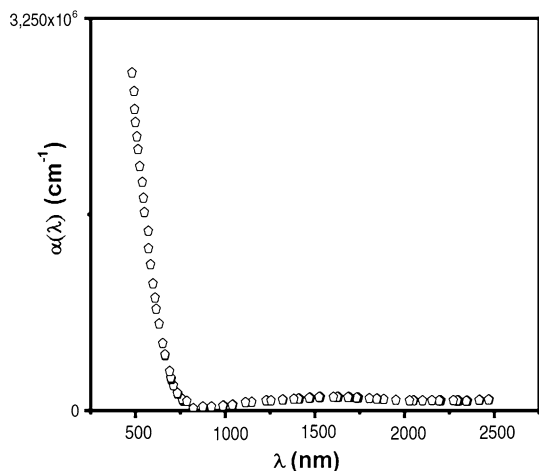
$$T = \frac{16 n_s (n^2 + k^2) \exp(-\alpha d)}{\left[(1+n)^2 + k^2\right]\left[(n_s + n)^2 + k^2\right]} \approx (1 - R)^2 \exp(-\alpha d)$$

(7)

$$\alpha \approx -\frac{1}{d} \ln\left[\frac{T}{(1-R)^2}\right].$$

(8)

The variation of α with the wavelength for the SnS(ZB) multilayers is shown in Fig. 4. It can be observed that zinc blend tin sulfide thin film exhibits a high absorption coefficient $> 1.5 \times 10^6$ cm^{-1} in the front absorption region 450–750 nm. SnS(ZB) multi films system are therefore suitable for absorber materials in solar cell [33]. In fact, the optical band gap is found to be equal to 1.76 eV [8].

Structural and chemical analysis of In$_2$S$_3$:Al (40%)

X ray spectrum of β-In$_2$S$_3$ (40% Al) thin layer deposited by CBD on SnO$_2$:F/glass is shown in Fig. 5. We point out the presence of three principal orientations toward (610), (551), and (311) planes, according to JCPDS Card no. 32-0456 of the cubic structure of β-In$_2$S$_3$ phase with oriented preferentially of crystallites toward (610) plan perpendicular to the substrate. The film is well crystallized but it

Fig. 2 The variations of refractive index "*n*" (**a**) and extinction coefficient "*k*" (**b**) of zinc blend tin sulfide elaborated by CBD on glass substrates after four (*a*), five (*b*), and six (*c*) depositions runs with wavelength in the 750–2500 nm domain
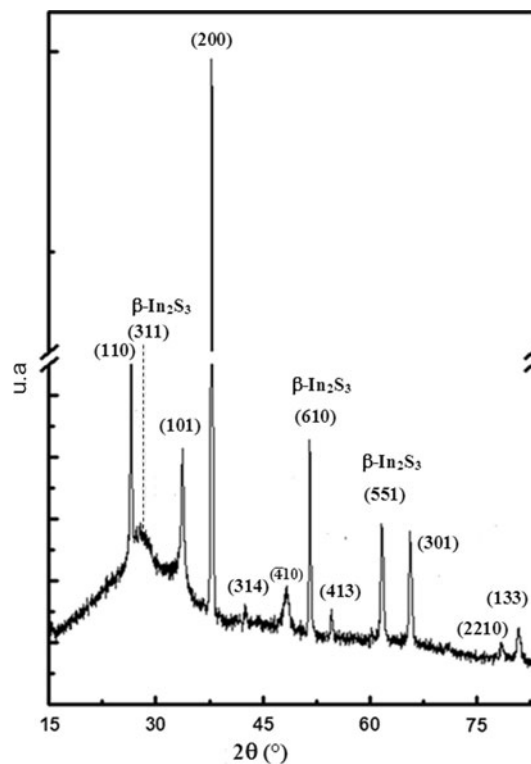
Fig. 4 The variation of absorption coefficient α with a wavelength λ for the SnS(ZB) thin films elaborated by CBD on glass substrates after six depositions runs

contains undesirable In_6S_7 and InS secondary phases corresponding to $(\bar{4}10)$ and (133) planes according to JCPDS Card nos. 19-0587 and no 65-1472. We also remark the existence of the tetragonal phase of Al_2S_3 assigned to (314) and (413), according to JCPDS Card no. 24-0014, as well as the hexagonal phase $AlInS_3$ corresponding to (2210) (JCPDS Card no. 71-0622). Planes assigned to (220), (110), and (301) indexes correspond to SnO_2:F thin layer deposited under β-In_2S_3:Al thin layers. In the same line, In_2S_3:Al (40%) thin films was also chemically analyzed by energy dispersive spectroscopy (EDS), we selected several points on the surface and the atomic percentage of Al, S, and In, values are gathered in Table 2. It is obviously shown that Al element exists which is consistent with X-ray diffraction analysis, Fig. 5.

The EDS results (Table 2) shows the existence of Al in the thin layers of β-In_2S_3 with a ratio equal to 0.1% value comparable to that found by Bhira et al. [34] who synthesized $In_{2-2x}Al_{2x}S_{3-3y}$ by the spray pyrolysis technique.

Optical analysis of cubic indium sulfide

The optical reflection–transmission of cubic indium sulfide grown for different ratios $y = \left(\left[Al^{3+} \right] / \left[In^{3+} \right] \right) = 0, 20, 30,$ and 40% are obtained with an NkdGen spectrophotometer at room temperature over 0.2–1.1 μm spectral range. It is clearly shown in Fig. 6 that Al content influences the optical properties of β-In_2S_3:Al thin films. In fact, the broadening and/or shift of the short wavelength absorption edge for larger Al inclusion can be ascribed both to the good optical quality and to a more ordered structure of β-In_2S_3:Al thin films. Furthermore, shift of the intrinsic absorption edge toward ultraviolet region leads to

Fig. 5 X-ray spectrum of the β-In_2S_3:Al (40%) thin layer deposited by CBD on SnO_2:F/glass substrate. Planes assigned to (200), (110), and (301) indexes correspond to the SnO_2:F thin layer above it β-In_2S_3:Al thin layers was grown
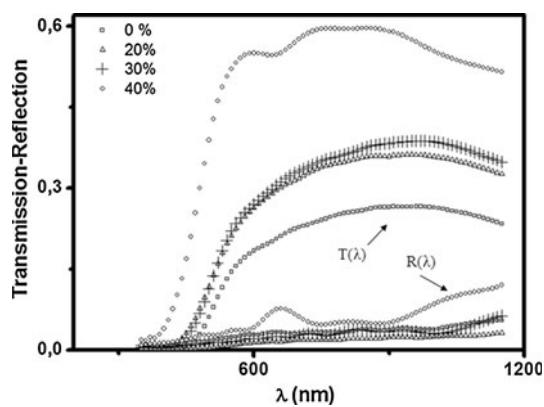
Table 2 EDS analysis of β-In_2S_3:Al multilayer thin film (four deposition runs) deposited on SnO_2:F/glass substrate for $y = \left(\left[Al^{3+} \right] / \left[In^{3+} \right] \right) = 40\%$

Elements analyzed	Al	S	In	S/In	$y = [Al^{3+}]/[In^{3+}]$ (%)
Results in atomic (%) (mean)	4.05	55.45	40.5	1.37	0.1

a maximal transmission coefficient in visible domain which allows us to use β-In_2S_3:Al as good optical window layer in photovoltaic devices. Moreover, in case of 40% Al contents we notice more clearly in Fig. 5 the presence of rather weak interference fringes on both $T(\lambda)$ and $R(\lambda)$ spectra which confirms that for this percentage content the indium sulfide thin films have uniform thickness as well as flat and smooth surfaces.

Layer thickness of the In_2S_3:Al multilayer is estimated by a Dektak[3] instrument that is a microprocessor-based contact stylus surface profiler used for making accurate measurements on vertical features ranging in height from 100 to 655000 angstroms. This instrument acquires data by slowly moving the sample beneath the diamond-tipped stylus. Vertical movements of the stylus are sensed by a
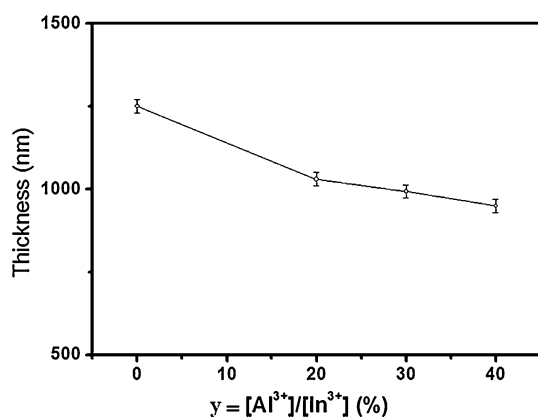
Fig. 6 Transmission–reflection of cubic indium sulfide multilayers elaborated by CBD with different Al content, $y = \left([Al^{3+}]/[In^{3+}]\right) = 0,\ 20,\ 30,$ and 40%

transducer, digitized, and stored in the memory for plotting and data manipulation. Figure 7 shows the average thickness of $In_2S_3:Al$ as a function of Al content. To check the thickness value, several points on the surface were selected and the thickness is measured for each of them. These measures are shifted by ±20nm; we concluded that the surface homogeneity was good at the scale of the Dektak[3] measurements accuracy. It is clearly shown in Fig. 7 that the film thicknesses of β-$In_2S_3:Al$ multilayer decrease from 1250 to 945 nm when the Al content increase from zero to 40%.

In the same way, the plot of αhv versus photon energy (hv) allows us to determine the absorption edge which can be expressed versus photon energy by the following equation:

$$\alpha hv = B(hv - E_g)^n, \tag{9}$$

where B is a parameter that depends on the transition probability and n is an index depending on the nature of the
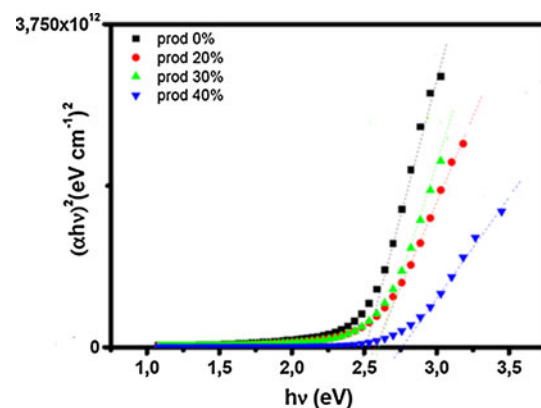
electronic transitions. $In_2S_3:Al$ multilayer system has a direct energy band gap $\left(n = \frac{1}{2}\right)$.

The extrapolation of linearly part of $(\alpha hv)^2$ versus hv intercepts on the hv axis and give a value of the energy band gap E_g, such plots are shown in Fig. 8. The straight lines imply that In_2S_3 (Al) samples have a direct energy band gap, which is a desirable result. In fact, at the absorption of a photon in the case of $h > E_g$, there will be creation of an electron–hole. The electron goes directly to the conduction band, this transition occurs between the maximum of valence band (VB) and the minimum of conduction band (CB). In the case of a direct band gap two extrema of VB and CB are located at the same value of wave vector "k" so at the same of the photon energy. Whereas in the case of an indirect gap these two extrema are located at different energies so the transfer of electron from the valence band to the conduction band is necessarily with the intervention of a phonon.

The variations of the optical energy band gap E_g values with Al inclusion are summarized in Table 3. This result is in agreement with the reported values [12, 35]. It is clear that the band gap E_g of indium sulfide multilayer system depends on the Al concentration. In fact, Al contents cause the increase of E_g, Table 3. This behavior may be due to the existence of Al_2S_3 and $AlInS_3$ undesirable phases as reveled by X-ray analysis, Fig. 5. Moreover, this result is in good agreement with those reported by Bhira et al. [34]. In fact, Bhira et al. showed that the optical band gap of $In_{2-2x}Al_{2x}S_{3-3y}$ thin film increases with Al concentration from 0 to 100%.

The refractive index "n" and extinction coefficient "k" of indium sulfide thin films grown for different contents of Al are determined from $T(\lambda)$ and $R(\lambda)$ spectra using the following expressions [29]:

Fig. 7 The average thickness of $In_2S_3:Al$ multilayers as a function of Al content, $y = \left([Al^{3+}]/[In^{3+}]\right) = 0,\ 20,\ 30,$ and 40%

Fig. 8 Plots of $(\alpha hv)^2$ versus hv of indium sulfide elaborated by CBD with different Al content, $y = \left([Al^{3+}]/[In^{3+}]\right) = 0,\ 20,\ 30,$ and 40%
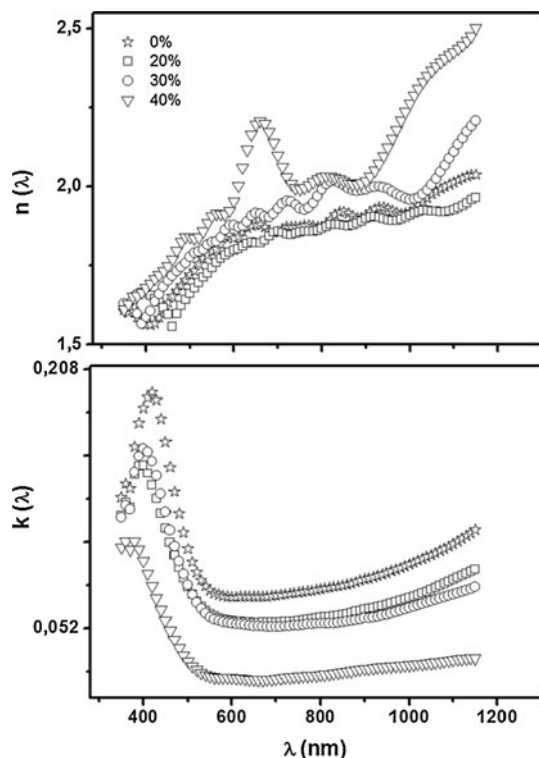
Table 3 Variation of energy band gap E_g of β-In$_2$S$_3$:Al multilayer thin film with different Al content, $y = \left([Al^{3+}]/[In^{3+}]\right) = 0$, 20, 30, and 40%

$y = [Al^{3+}]/[In^{3+}]$ (%)	0	20	30	40
E_g (eV)	2.51	2.57	2.59	2.76

$$n = \frac{1 + [1 - \left(\frac{1-R}{1+R}\right)^2(1 + k^2)]^{1/2}}{\left(\frac{1-R}{1+R}\right)} \qquad (10)$$

$$k = \frac{\lambda}{4\pi e}\ln\left[\frac{(1-R)^2}{T}\right]. \qquad (11)$$

Figure 9 shows the plot of "n" and "k" as a function of wavelength (λ). We note that for $y = \left([Al^{3+}]/[In^{3+}]\right) = 40\%$, "$n$" and "$k$" varied in the range of 1.61–2.5 and 0.03–0.1, respectively. Furthermore, β-In$_2$S$_3$:Al thin films grown for $y = \left([Al^{3+}]/[In^{3+}]\right) = 40\%$ show high refractive index and lower extinction coefficient values in the visible domain, which indicates good optical quality. This last finding is in agreement with those reported by Trigo et al. [35].

Fig. 9 Plot of (n) and (k) of β-In$_2$S$_3$:Al grown for $y = [Al^{3+}]/[In^{3+}] = 0$, 20, 30, and 40% as a function of wavelength λ

Conclusions

Zinc blend tin sulfide and cubic indium sulfide have been prepared by CBD technique.

The number of deposition runs influences the physical properties of CBD deposited SnS thin layer. It is found that better thickness of SnS thin film 455 nm is obtained after six depositions run estimated by envelope method which is correlated to the experimental value given in our previously study [8]. Using the theory of Manifacier et al. in transparency region the optical properties were found for SnS material. The refractive index "n" value was found to be of the order of 2.5. SnS thin films exhibits a high absorption coefficient $> 1.5 \times 10^6$ cm^{-1} in the front absorption region 450–750 nm and low value of extinction coefficient which is a qualitative indication of excellent surface smoothness and homogeneity of the films. Therefore, SnS(ZB) thin films are suitable for absorber layers in solar cell. This indicates good optical quality which permits to use this binary material as absorber layer in photovoltaic device.

Moreover, we note that Al content affects the physical properties of β-In$_2$S$_3$ CBD thin layer. In fact, β-In$_2$S$_3$:Al grown for $y = [Al^{3+}]/[In^{3+}] = 40\%$ show a higher refractive index, the transmission upper to 55%, the wider band gap is close to 2.76 eV, and a lower extinction coefficient in the visible domain. This indicates good optical quality of these films which allows us to use them as window layers in photovoltaic devices.

Study is also in progress to incorporate these layers in some possibly future photovoltaic devices such as: SnS/In$_2$S$_3$:Al (40%)/SnO$_2$:F, SnS:Cu/In$_2$S$_3$:Al (40%)/SnO$_2$:F, and SnS:In/In$_2$S$_3$:Al (40%)/SnO$_2$:F.

References

1. Ramakrishna Reddya KT, Koteswara Reddya N, Miles RW (2006) Sol Energy Mater Sol Cells 90:3041
2. Ghosh B, Das M, Banerjee P, Das S (2008) Sol Energy Mater Sol Cells 92:1099
3. Avellaneda D, Guadalupe D, Nair MTS, Nair PK (2007) Thin Solid Films 515(15):5771
4. Thangaraju B, Kaliannan P (2000) J Phys D Appl Phys 33:1054
5. Koteswara Reddy N, Ramakrishna Reddy KT (1998) Thin Solid Films 325(1–2):4
6. Yue GH, Peng DL, Yan PX, Wang LS, Wang W, Luo XH (2009) J Alloys Compd 468(1–2):254
7. Ghosh B, Das M, Banerjee P, Das S (2008) Appl Surf Sci 254(August 20):6436

8. Akkari A, Guasch C, Kamoun-Turki N (2010) J Alloys Compd 490:180

9. Avellaneda D, Nair MTS, Nair PK (2009) Thin Solid Films 517:2500

10. Manifacier JC, Gasiot J, Fillard JP (1976) J Phys E: Scientific Instruments 9

11. Bessergenev VG, Bessergenev AV, Ivanova EN, Kovalevskaya YA (1998) J Solid State Chem 137:6

12. El-Nahass MM, Khalifa BA, Soliman HS, Seyam MAM (2006) Thin Solid Films 515:1796

13. Womes M, Jumas JC, Olivier-Fourcade J (2004) Solid State Commun 131:257

14. Yoosuf R, Jayaraj MK (2005) Sol Energy Mater Sol Cells 89:85

15. Dong G, Tao H, Chu S, Wang S, Zhao X, Gong Q, Xiao X, Lin C (2007) Opt Commun 270:373

16. Amlouk M, Ben Said MA, Kamoun N, Belgacem S, Brunet N, Barjon D (1999) Jpn J Appl Phys Part 1 38:26

17. Shen S, Guo L (2006) J Solid State Chem 179:2629

18. Strohm A, Eisenmann L, Gebhardt RK, Harding A, Schlotzer T, Abou-R Ras D, Schock HW (2005) Thin Solid Films 480–481:162

19. Asikainen T, Ritala M, Leskela M (1994) Appl Surf Sci 82:122

20. Sysoev BI, Linnik VD, Titov SA, Kordenko OI (1994) Phys Status Solidi A 143:71

21. Braunger D, Hariskos D, Waltre T, Schock HW (1996) Sol Energy Mater Sol Cells 40:97

22. Amlouk M, Belgacem S, Kamoun N, El Houichet H, Bennaceur R (1994) Ann Chim (Paris) 19:49

23. Dalas E, Sakkopoulos S, Vitoratos E, Maroulis G, Kobotiatis L (1993) J Mater Sci 28:5456. doi:10.1007/BF00367815

24. Bessergenev VG, Ivanova EN, Kovalerskaya YA, Gromilov SA, Kirichenko VN, Larionov SV (1996) Inorg Mater (Translation of Neorg Mater) 32:592

25. Yahmadi B, Kamoun N, Bennaceur R, Mnari M, Dachraoui M, Abdelkrim K (2005) Thin Solid Films 473:201

26. Yahmadi B, Kamoun N, Guasch C, Bennaceur R (2011) Mater Chem Phys 127:239

27. Kamoun N, Belgacem S, Amlouk M, Bennaceur R, Bonnet J, Touhari F, Nouaoura M, Lassabatere L (2001) J Appl Phys 89(5):2766

28. Haleem AMA, Ichimura M (2009) Jpn J Appl Phys 48:035506

29. Belgacemet S, Bennaceur R (1990) Rev Phys Appl 25:1245

30. Pramanik P, Basu PK, Biswas S (1987) Thin Solid Films 150:269

31. Subramanian B, Sanjeeviraja C, Jayachandran M (2001) Mater Chem Phys 71:40

32. Koteeswara Reddy N, Ramakrishna Reddy KT (2007) Mater Chem Phys 102:13

33. Avellaneda D, Nair MTS, Nair PK (2008) J Electrochem Soc 155(7):D517

34. Bhira L, Ben Nasrallah T, Bernède JC, Belgacem S (2001) Mater Chem Phys 72:320

35. Trigo JF, Asenjo B, Herrero J, Gutiérrez MT (2008) Sol Energy Mater Sol Cells 92:1145